https://doi.org/10.5194/acp-2020-792
Preprint. Discussion started: 25 August 2020

Atmospheric Chemistry and Physics Discussions

Measurement report: Effects of photochemical aging on the formation and evolution of summertime secondary aerosol in Beijing

Tianzeng Chen[a], Jun Liu[a, c], Qingxin Ma[a, b, c, *], Biwu Chu[a, b, c], Peng Zhang[a], Jinzhu Ma[a, b, c], Yongchun Liu[d], Cheng Zhong[a, c], Pengfei Liu[a], Yafei Wang[e], Yujing Mu[a, b, c], Hong He[a, b, c]

[a] State Key Joint Laboratory of Environment Simulation and Pollution Control, Research Center for Eco-Environmental Sciences, Chinese Academy of Sciences, Beijing 100085, China

[b] Center for Excellence in Regional Atmospheric Environment, Institute of Urban Environment, Chinese Academy of Sciences, Xiamen 361021, China

c University of Chinese Academy of Sciences, Beijing 100049, China

[d.] Beijing Advanced Innovation center for Soft Matter Science and Engineering, Beijing University of Chemical Technology, Beijing 100029, China

[e.]Beijing Institute of Petrochemical Technology, Beijing 102617, China

Corresponding author: qxma@rcees.ac.cn (Qingxin Ma)

https://doi.org/10.5194/acp-2020-792
Preprint. Discussion started: 25 August 2020

Atmospheric Chemistry and Physics Discussions

Abstract

Atmospheric submicron aerosols have a great effect on air quality and human health, while their formation and evolution processes are still not fully understood. Herein, the crucial role of atmospheric oxidation capacity, as characterized by OH exposure dose in the formation and evolution of secondary submicron aerosols, was systematically investigated based on a highly time-resolved chemical characterization of PM_1 in a southern suburb of Beijing in summertime from 25th July to 21st August 2019. The averaged concentration of PM_1 was 19.3 ± 11.3 μg m^{-3}, and nearly half (48.3%) of the mass was organic aerosols (OA) during the observation period. The equivalent photochemical age (t_a) estimated from the ratios of toluene to benzene was applied to characterize the OH exposure dose of the air mass. The relationships of NR-PM_1 species, OA factors (i.e., one hydrocarbon-like (HOA) and three oxygenated (LO-OOA, SV-OOA and MO-OOA) organic aerosol factors) and elemental compositions (e.g., H/C, O/C, N/C, S/C, OM/OC, and OSc) to t_a were analyzed in detail. It was found that higher PM_1 concentration accompanied longer t_a, with an average increase rate of 0.8 μg m^{-3} per hour. Meanwhile, the formation of SO_4^{2-} and MO-OOA were most sensitive to the increase in t_a, and their contributions to PM_1 were enhanced from 19% to 27% and from 27% to 48%, respectively, as t_a increased from 9.4 h to 19.6 h. In addition, OSc and the ratios of O/C and OM/OC increased with the increase in t_a. These results indicated that photochemical aging is a key factor leading to the evolution of OA and the increase of PM_1 in summertime.

Keywords

PM_1; Aerosol mass spectrometer; Photochemical age; Atmospheric oxidation capacity; Positive matrix factorization

https://doi.org/10.5194/acp-2020-792
Preprint. Discussion started: 25 August 2020

Atmospheric Chemistry and Physics Discussions

1 Introduction

Fine particulate matter ($PM_{2.5}$) is one of the major atmospheric environmental problems owing to its effects on air quality, human health, and climate (IPCC, 2013; Davidson et al., 2005; Molina and Molina, 2004). In recent years, the $PM_{2.5}$ concentration in China exhibited a significant decrease with the implementation of the measures and strict policies in the Air Pollution Prevention and Control Action Plan (Action Plan) (Zhang et al., 2019). However, the nationwide annual average concentration of $PM_{2.5}$ is still greater than the standard of the World Health Organization (WHO) and $PM_{2.5}$ is the primary pollutant in many regions, especially in the North China Plain (NCP). Beijing, one of the most polluted megacities in the NCP, is also facing severe $PM_{2.5}$ pollution. The annual mean concentration in Beijing was 51 μg m^{-3} in 2018 (http://sthjj.beijing.gov.cn/), which significantly exceeds the Chinese National Ambient Air Quality Standard (annual average of 35 μg m^{-3}) and the WHO Standard (annual average of 10 μg m^{-3}). Continuing to reduce the $PM_{2.5}$ concentration is an important issue in improving the air quality in Beijing.

It has been well recognized that secondary aerosols (SA), including secondary inorganic aerosol (SIA) and secondary organic aerosol (SOA), are the crucial constituents (30-77%) of $PM_{2.5}$ (Xie et al., 2020; An et al., 2019; Sun et al., 2016a; Guo et al., 2014; Huang et al., 2014). However, the formation and evolution mechanism of SA is still not well understood, mainly due to multiple precursors, complex formation processes, and meteorological conditions (Chen et al., 2020; Duan et al., 2020; Chen et al., 2019a; Duan et al., 2019; Hua et al., 2018; Li et al., 2018a; Tie et al., 2017; Sun et al., 2015). Therefore, from the perspective of precise $PM_{2.5}$ control, in-depth understanding of the processes related to SA formation and evolution is crucial.

The Aerodyne high-resolution time-of-flight aerosol mass spectrometer (HR-ToF-AMS) has

https://doi.org/10.5194/acp-2020-792
Preprint. Discussion started: 25 August 2020


Atmospheric Chemistry and Physics Discussions

the advantage of real-time measurement of non-refractory submicron aerosol (NR-PM_1) with high time resolution and sensitivity, compared to filter measurements (DeCarlo et al., 2006). As a result, HR-ToF-AMS measurements have been widely employed for illustrating the formation and evolution of PM in China (Chen et al., 2020; Xu et al., 2019b; Wu et al., 2018; Ge et al., 2017; Ye et al., 2017; Qin et al., 2016; Sun et al., 2016a; Huang et al., 2015; Li et al., 2015; Xu et al., 2014; Li et al., 2013). Many previous field observation studies have inspected the formation mechanism and process of SA (Huang et al., 2019; Shi et al., 2019; Sun et al., 2018a,b; Wang et al., 2017; Xu et al., 2017; Cheng et al., 2016; Wang et al., 2016; Sun et al., 2016b; Sun et al., 2014). For example, studies showed that an aqueous-phase process could be an important pathway in the formation of SO_4^{2-} (Elser et al., 2016) and NO_3^- (Duan et al., 2020). However, most recent studies suggested that SO_4^{2-} formation was also associated with a photochemical process, which is closely related to the meteorological conditions, especially in summertime (Chen et al., 2020; Duan et al., 2019). In terms of SOA, its contribution to fine particles was reported to be as important as SIA during haze events in China (Huang et al., 2014). However, the formation mechanism of SOA is much less understood compared to SIA because SOA consist of various organic species with different oxidation degrees. Meanwhile, based on the organics database measured by HR-ToF-AMS, positive matrix factorization (PMF) analysis, one receptor model (Paatero and Tapper, 1994), has been employed to distinguish and quantify multiple OA factors (Hu et al., 2016; Sun et al., 2016b). Studies have found that photochemical and aqueous-phase processes played different roles in the evolution of SOA, which depended on the level of atmospheric oxidation capacity (e.g., total oxidant O_x (= O_3 + NO_2)), relative humidity (RH), seasons and regions (Chen et al., 2020; Feng et al., 2019; Wang et al., 2017; Xu et al., 2017). For example, an aqueous-phase process was reported to have a significant

https://doi.org/10.5194/acp-2020-792
Preprint. Discussion started: 25 August 2020


Atmospheric Chemistry and Physics Discussions

effect on the formation of less-oxidized oxygenated OA (LO-OOA) and more-oxidized oxygenated OA (MO-OOA) at low levels of atmospheric oxidation capacity in wintertime Baoji, Shaanxi (Wang et al., 2017). However, Xu et al. (2017) demonstrated that the formation of MO-OOA was significantly dominated by the aqueous-phase process, while LO-OOA was closely correlated with the photochemical process in urban Beijing (Xu et al., 2017). These inconsistences highlight the necessity of studying the role of atmospheric chemical processes in the formation and evolution of different types of SOA.

Previous studies have revealed some important factors (e.g., seasonal variation, meteorological factors, and pollution degree) that influence the formation and evolution of PM_1 in Beijing, based on AMS observations (Hu et al., 2016; Sun et al., 2013b; Sun et al., 2012, Sun et al., 2013a, and Zhang et al., 2014, respectively). Nevertheless, it should be pointed out that as the $PM_{2.5}$ concentration decreases, the ozone (O_3) concentration increases year by year (Li et al., 2019b; Zhang et al., 2019). O_3 has become the primary air pollutant in summertime in the NCP and has caused the enhancement of atmospheric oxidation capacity. Therefore, there is an urgent need to investigate the impact of these changes on the atmospheric oxidation capacity and the formation and evolution of PM_1. Moreover, it should be noted that most previous AMS observations in Beijing were carried out in urban areas (Duan et al., 2020; Xu et al., 2019b; Wang et al., 2018; Li et al., 2017; Xu et al., 2017; Hu et al., 2016; Zhang et al., 2014; Sun et al., 2013a,b; Sun et al., 2012; Liu et al., 2012; Huang et al., 2010; Sun et al., 2010), while few studies were deployed in suburban areas (Chen et al., 2020; Li et al., 2019a). Considering the different meteorological factors and emission sources, the contribution of different formation and evolution pathways to PM_1 in urban and suburban areas could be different.

https://doi.org/10.5194/acp-2020-792
Preprint. Discussion started: 25 August 2020


Atmospheric Chemistry and Physics Discussions

In this study, a field observation, mainly using HR-ToF-AMS, was conducted from 25th July to 21st August 2019 in a typical suburban site in Daxing District, which is the south gate of Beijing. The observation site lies in the air pollution transport channel between Beijing and Hebei province. Based on the measurement results of a series of gas- and particle-phase monitoring instruments, the chemical composition of NR-PM_1, elemental ratios, and source categories of OA were analyzed. Moreover, the formation and evolution of secondary aerosols were elucidated. Specifically, the effects of atmospheric oxidation capacity, which was characterized using the equivalent photochemical age (t_a), on the formation of secondary aerosols were discussed.

2 Experimental methods

2.1 Sampling site

The online field observation was carried out in the top floor of a building (9th, ~27 m above the ground) at the Qingyuan campus of Beijing Institute of Petrochemical Technology in Daxing District (39.73°N, 116.33°E) from 25th July to 21st August 2019. The site is located between the 5th ring road and the 6th ring road in the south of Beijing and is a typical suburban site. Additionally, there is no additional source of pollution except for two adjacent streets (i.e., Xinghua Street and Qingyuan Street, with a distance ~600 m).

2.2 Instrumentation

The mass concentration and chemical composition of NR-PM_1 were simultaneously measured by a HR-ToF-AMS (Aerodyne Research Inc. USA). The detailed principles of HR-ToF-AMS can be found elsewhere (DeCarlo et al., 2006). Briefly, the aerosols are sampled through a critical orifice and then concentrated into a narrow beam via an aerodynamic lens. The size of aerosol is determined using the flight time of particles to the thermal vaporization and ionization chamber. Then the

https://doi.org/10.5194/acp-2020-792
Preprint. Discussion started: 25 August 2020


Atmospheric Chemistry and Physics Discussions

aerosols are successively vaporized by a heated surface (~600 °C), ionized by electron ionization (EI, 70 eV), and detected by a mass spectrometer detector. During this field observation, the HR-ToF-AMS was operated under alternation of two modes, i.e., 2 min V mode and 2 min W mode. Meanwhile, routine quality assurance and quality control procedures, mainly including the calibration of inlet flow, ionization efficiency (IE), and aerosol sizing, were carried out regularly every week according to the standard protocols, using pure dry mono-dispersed 300 nm NH_4NO_3 aerosols (Chen et al., 2019b; Drewnick et al., 2005) to guarantee the credibility of the HR-ToF-AMS results. The size distribution and number concentration of aerosols with a mobility diameter from 13.6 nm to 736.5 nm were also measured by a custom-built scanning mobility particle sizer (Model 3082 equipped with 3776 CPC, TSI, USA).

The gas-phase species including NO_x, NO_y, SO_2, O_3, and CO were measured in real time by a series of Thermo analyzer (Model 42i-TL, Model 42i-NO_y, Model 43i, Model 49i, Model 48i, respectively). The volatile organic compounds (VOCs) (e.g., benzene and toluene) concentrations were measured on-line using a vacuum ultraviolet single-photon ionization time-of-flight mass spectrometer (SPIMS-3000, Guangzhou Hexin Analytical Instrument Co., Ltd., China). These instruments were calibrated periodically with the corresponding standard gas to ensure the accuracy of the observation data. In addition, two Apresys Temperature Humidity Data Loggers (179-UTH, Apresys, USA) were also used to measure the meteorological parameters including temperature (T) and RH.

2.3 Data analysis

2.3.1 HR-ToF-AMS data analysis

The standard analysis software tool (SQUIRREL, Version 1.57I and PIKA, Version 1.16I)

https://doi.org/10.5194/acp-2020-792
Preprint. Discussion started: 25 August 2020

Atmospheric Chemistry and Physics Discussions

written in Igor Pro (Version 6.37, Wavemetrics Inc., USA) was used to analyze the HR-ToF-AMS data. In order to obtain the quantitative mass concentrations of different species (i.e., OA, SO_4^{2-}, NO_3^-, NH_4^+, and Cl^-), and considering that the aerosols were almost neutral and had been dried before entering into the HR-ToF-AMS inlet, the collection efficiency factor (CE) was determined according to the following equation (Middlebrook et al., 2012):

$$CE = \max(0.45, 0.0833 + 0.9167 \times ANMF) \quad (1)$$

where ANMF is the mass fraction of NH_4NO_3 in NR-PM_1. The default relative ionization efficiency (RIE) values were used for OA (1.4), NO_3^- (1.1), and Cl^- (1.3) (Jimenez et al., 2003). As for NH_4^+ and SO_4^{2-}, their RIE values were determined using the pure dry mono-dispersed NH_4NO_3 and $(NH_4)_2SO_4$ aerosols to be 4.0 and 1.2, respectively.

Elemental analysis (EA) was also executed using the "Improved-Ambient" method (Canagaratna et al., 2015) to obtain the hydrogen-to-carbon ratio (H/C), oxygen-to-carbon ratio (O/C), and organic-mass to organic-carbon ratio (OM/OC), as well as elemental ratios of N/C and S/C. The average carbon oxidation state (OSc) can be approximated by 2×O/C-H/C and is a metric describing the oxidation degree of atmospheric OA (Kroll et al., 2011).

2.3.2 PMF analysis of OA

Source apportionment of OA was executed using the PMF model to analysis the HR-ToF-AMS mass spectral data to identify the main organic components and their sources (Zhang et al., 2011). PMF, as a bilinear receptor model, can be expressed as the following equation (Paatero, 1997; Paatero and Tapper, 1994):

$$\mathbf{X} = \mathbf{GF} + \mathbf{E} \quad (2)$$

where **X** is the observed data matrix with dimensions of n × m. **G** is the factor contribution matrix of dimensions n × p, **F** is the factor profile matrix of dimensions p × m, and **E** is the matrix of

https://doi.org/10.5194/acp-2020-792
Preprint. Discussion started: 25 August 2020

Atmospheric Chemistry and Physics Discussions

residuals with dimensions of n × m. n, m, and p are the number of samples, species, and factors, respectively.

A least-squares fitting method was used to minimize the object function Q, which is defined as the sum of the squared residuals (e_{ij}) weighted by their degree of measurement uncertainty (σ_{ij}).

$$Q=\sum_{i=1}^{n}\sum_{j=1}^{m}(e_{ij}/\sigma_{ij})^2$$

In our study, the PMF software tool (PMF Evaluation Tool, PET, version 2.06) (Ulbrich et al., 2009) written in Igor Pro (Version 6.37, Wavemetrics Inc., USA) was used to analyze the HR-ToF-AMS mass spectra (*m/z* 12-170). The detailed steps have been expressed in Zhang et al. (2011). According to the values of the signal-to-noise ratios (SNR), *m/z* with SNR in a range of 0.2-2 were weak variables and down-weighted 2 times, and *m/z* with SNR less than 0.2 were bad variables and directly removed. As for duplicate information, *m/z* 44 (CO_2) and related *m/z* values (including 16 (O), 17 (HO), 18 (H_2O), and 28 (CO)) were also down-weighted. Then PMF was run for a range of number of factors (from 1 to 5) and rotational parameters (FPEAK) (from -1 to 1 with a step of 0.2). After considering multiple criteria, including mass spectral features, diurnal patterns, correlation with external tracers, and temporal variations (Zhang et al., 2011), the best number of factors was determined to be 4, including one hydrocarbon-like OA (HOA) and three oxygenated organic aerosol factors (LO-OOA, SV-OOA and MO-OOA). The corresponding mass spectra, time series, and diurnal variation, which are similar to our previous results observed in the same site during summertime 2018 (Chen et al., 2020), are given in Fig. S1.

2.3.3 Photochemical age

In the ambient air, the reaction of benzene and toluene with O_3 and NO_3 radicals is very slow, with reaction rate on the order of $<10^{-20}$ and $<10^{-16}$ cm^3 $molecule^{-1}$ s^{-1}, respectively (Atkinson and

https://doi.org/10.5194/acp-2020-792
Preprint. Discussion started: 25 August 2020

Atmospheric Chemistry and Physics Discussions

Arey, 2003), which is significantly lower than the reaction rate with OH radicals (10^{-12} cm^3 $molecule^{-1}$ s^{-1}). Thus, their degradation is dominated by reaction with OH radicals. Meanwhile, the reaction rate of toluene with OH radicals is about five times that of benzene. Therefore, their degradation rates in the ambient air are significantly different after being exhausted from an emission source, which would lead to an observable change in their concentration ratio. Consequently, the ratio of toluene to benzene is typically used to study the photochemical aging process of localized air masses (Yuan et al., 2012; Parrish et al., 2007; de Gouw et al., 2005; Gelencsér et al., 1997; McKeen et al., 1996).

In this study, the equivalent photochemical age (t_a) was calculated to characterize the OH exposure dose of the air mass, as expressed in the following equation:

$$t_a = \frac{1}{[OH](k_{toluene} - k_{benzene})} \times \left[\ln\left(\frac{[toluene]}{[benzene]}\right)_0 - \ln\left(\frac{[toluene]}{[benzene]}\right)\right]$$

where [OH] is the average OH concentration in the ambient air and is assumed as 5.2×10^6 molecule cm^{-3}, which was the average daytime ambient OH concentration observed in summer of Beijing (Yang et al., 2017). $k_{toluene}$ and $k_{benzene}$ are the rate constants for the reactions of OH with toluene (5.63×10^{-12} cm^3 $molecule^{-1}$ s^{-1}) and benzene (1.22×10^{-12} cm^3 $molecule^{-1}$ s^{-1}), respectively (Atkinson and Arey, 2003). $\left(\frac{[toluene]}{[benzene]}\right)_0$ is the emission concentration ratio of toluene and benzene before aging in the atmosphere, and was determined to be 3.3 (Fig. S2, in the Supplement). $\frac{[toluene]}{[benzene]}$ is the measured concentration ratio of toluene and benzene, which is given in Fig. S3a. The diurnal variation of calculated t_a (Fig. S3b) followed a similar diurnal trend of OH radicals observed in summertime of Beijing, which had a higher level at noon (Tan et al., 2019). Therefore, this method can provide useful information on the photochemical process in the atmosphere (Yuan

https://doi.org/10.5194/acp-2020-792
Preprint. Discussion started: 25 August 2020

Atmospheric Chemistry and Physics Discussions

et al., 2012; Parrish et al., 2007; de Gouw et al., 2005; McKeen et al., 1996).

3 Results and discussion

3.1 Chemical compositions of PM_1

The time series of mass concentrations of NR-PM_1 species (i.e., OA, NO_3^-, SO_4^{2-}, NH_4^+, and Cl^-) and their relative contributions are summarized in Fig. 1. During this field observation, the hourly mass concentrations of NR-PM_1 was in the range of 2.2-64.3 μg m^{-3}, with an average of 19.3 ± 11.3 μg m^{-3}, which is close to those observed in a suburb of Beijing in summer 2016 (14.2 ± 9.4 μg m^{-3}, Li et al., 2019a) and summer 2018 (24.1 ± 18.0 μg m^{-3}, Chen et al., 2020). However, this averaged PM_1 concentration was much lower than those observed in urban Beijing in summertime, such as 80 ± 40.6 μg m^{-3} in 2006 (Sun et al., 2010), 63.1 μg m^{-3} in 2008 (Huang et al., 2010), 50 ± 30 μg m^{-3} in 2011 (Sun et al., 2012), and 37.5 ± 31.0 μg m^{-3} in 2012 (Hu et al., 2017). Meanwhile, among all species in NR-PM_1, OA contributed the most (48.3%), indicating the dominant role of OA in summertime PM_1 pollution (Chen et al., 2020; Hu et al., 2016; Sun et al., 2015; Zhang et al., 2014). Moreover, the largest daily contribution of OA (> 80%) was observed during the clean period, with PM_1 concentration less than 20 μg m^{-3} (e.g., from 16th August to 18th August 2019, Fig. 1b). With further improvement in air quality, PM_1 concentrations would decrease in the future. Then, the contribution of OA in PM_1 is likely to increase. On the other hand, SIA accounted for 51.7% of NR-PM_1, in which SO_4^{2-} was the largest contributor (23.2%), followed by NO_3^- (14.3%), NH_4^+ (13.4%), and Cl^- (0.8%). Similar relative contributions of these species were also observed in a suburb of Beijing in summer 2016, where OA contributed a mass fraction of 42-71%, followed by SO_4^{2-} (15-27%), NO_3^- (6-22%), NH_4^+ (8-13%), and Cl^- (0.3-0.6%) (Li et al., 2019a). By comparison, NR-PM_1 in urban Beijing in summertime had relatively low contribution of OA (33-40%) and high

https://doi.org/10.5194/acp-2020-792
Preprint. Discussion started: 25 August 2020

Atmospheric Chemistry and Physics Discussions

contribution of SIA (58-65%) (Hu et al., 2017; Sun et al., 2012; Huang et al., 2010; Sun et al., 2010), which may be due to the difference in the emissions of gaseous precursors (e.g., SO_2 and NO_x) and their conversion ratio to SIA (Li et al., 2020; Hu et al., 2017). Meanwhile, the inorganic SO_4^{2-}, NO_3^-, and Cl^- could be well neutralized by NH_4^+ during this field observation since there is an extremely good linear relationship between $NO_3^-+2\times SO_4^{2-}+Cl^-$ and NH_4^+ (R^2 = 0.998, slope = 0.992 ± 0.002, Fig. S4, in the Supplement). This implied the significant contribution of gaseous NH_3 to the formation of SIA and $PM_{2.5}$. Therefore, NH_3 emission control in China should be strengthened in the future to mitigate PM pollution (Liu et al., 2019b).

Figure 1 also presents the time series of total oxidant ($O_x = O_3 + NO_2$) and photochemical age (t_a). In this study, t_a and O_x can be used to characterize the photochemical aging process undergone and the total oxidant present in the ambient atmosphere, respectively. As shown in Fig. 1c, t_a showed a similar evolutionary trend to that of O_x during this summertime observation, which is consistent with the formation process of photochemical smog in the presence of NO_x, VOCs, and sunlight. It is well known that the photochemical aging process of VOCs can enhance the formation of organic peroxy radical (RO_2) and hydroperoxy (HO_2), which will then accelerate the cycle of NO_x and the formation of O_3 in the atmosphere. Consequently, longer aging time (t_a) always corresponds to a higher concentration of O_3 and stronger atmospheric oxidation during summertime.

https://doi.org/10.5194/acp-2020-792
Preprint. Discussion started: 25 August 2020

Atmospheric Chemistry and Physics Discussions

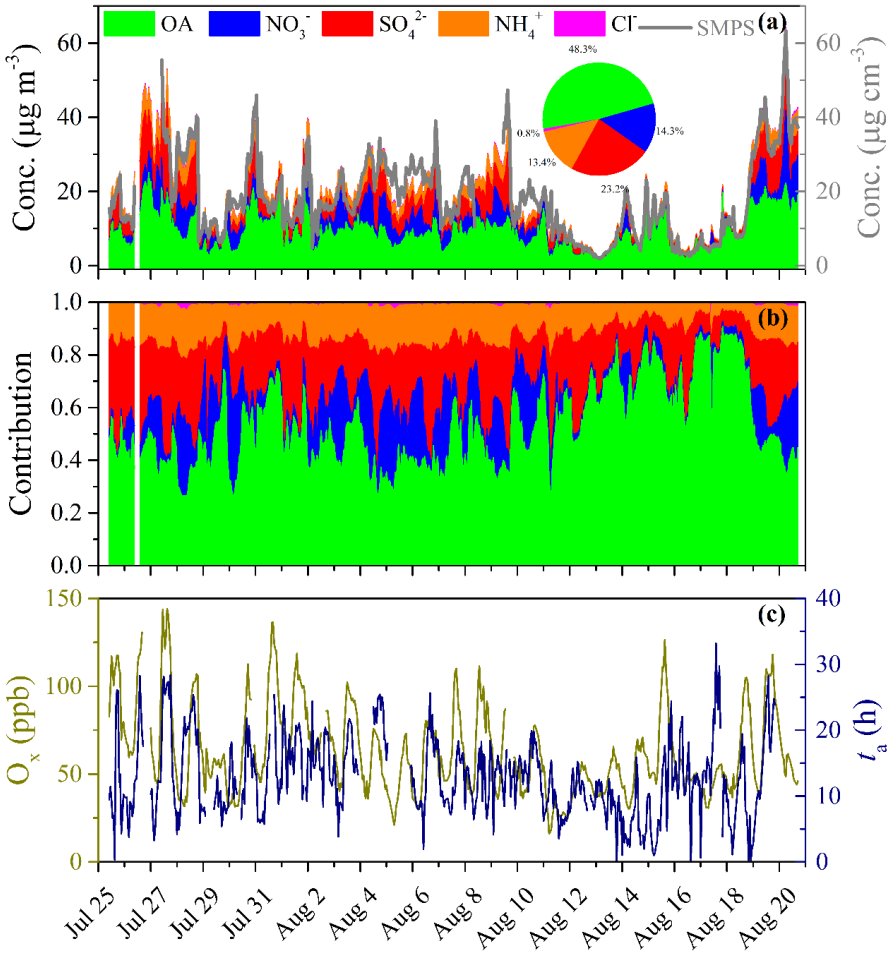

Figure 1. Overview of time series of (a) concentrations of NR-PM_1 species derived from HR-ToF-AMS (left y axis) and SMPS (right y axis), (b) relative contributions of NR-PM_1 species, and (c) concentration of total oxidant (O_x = O_3 + NO_2) and photochemical age (t_a) during this field observation.

3.2 Role of t_a in aerosol formation and composition

In order to evaluate the effect of the photochemical aging process on PM_1 concentrations, the relationships among t_a, O_x, OA concentration, and binned PM_1 concentration were analyzed and shown in Fig. 2. Both t_a and O_x simultaneously rose with the increasing concentration of PM_1. This

https://doi.org/10.5194/acp-2020-792
Preprint. Discussion started: 25 August 2020


Atmospheric Chemistry and Physics Discussions

suggested that the photochemical aging process was closely related to the PM pollution level, and that the photochemical process becomes more intensive with the increase of VOCs and O_x at higher PM_1 concentrations. In addition, the similar evolutionary trends of t_a and O_x during this summertime observation further confirmed that they are closely correlated. Meanwhile, with the increase in t_a, concentrations of PM_1 and O_3 increased simultaneously (Fig. S5, in the Supplement), which indicated that the formation of PM_1 and O_3 were both positively correlated with the photochemical aging process during this summer observation. One reason is that high temperature observed at elevated t_a levels (Fig. S6) increases the emission rates of biogenic VOCs (Fu et al., 2010), which could promote the formation of O_3 and PM_1 (Li et al., 2019c; Schnell and Prather, 2017). Considering that the concentration of NO_x decreased with increasing t_a (Fig. S6), this implied that the formation of O_3 is in the VOC-sensitive regime during this observation. Under this condition, increased VOCs will enhance the reactions between VOCs and OH, resulting in high production of RO_2 and O_3 locally (Li et al., 2018b). The concentration of OA also persistently increased with t_a, which was consistent with the fact that SOA (predominant species in OA) mainly originated from the photochemical process of VOCs (Fan et al., 2020; Fu et al., 2014; Hallquist et al., 2009). Higher production of RO_2 will be beneficial to the formation of low volatility species and new particle formation (NPF) (Garmash et al., 2020; Tröstl et al., 2016), and then promote the formation of SOA through gas-particle partitioning (Odum et al., 1996). These results implied that the formation and evolution of PM pollution as well as OA was greatly dependent on the photochemical aging process and total oxidant present during the summertime, which need to be deeply explored to understand the growth of PM_1.

https://doi.org/10.5194/acp-2020-792
Preprint. Discussion started: 25 August 2020

Atmospheric Chemistry and Physics Discussions

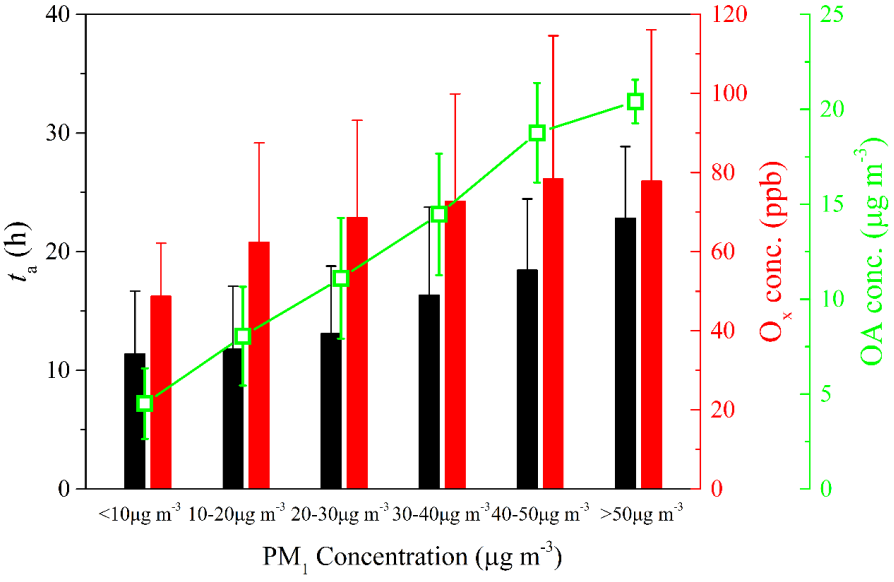

Figure 2. Relationship between PM_1 concentration and photochemical age (t_a), total oxidant (O_x), as well as OA concentration during this field observation. The data are binned according to PM_1 concentration (10 μg m^{-3} increment).

To further investigate the role of t_a in aerosol formation, all NR-PM_1 species and OA factors were normalized to HOA to exclude the accumulation and/or dilution effects in the atmosphere, and the corresponding ratios as a function of t_a are given in Fig. 3. Although the HOA emissions vary throughout the day and might bring some uncertainty, Sun et al. (2013a) indicated that this uncertainty might be reduced and become insignificant when these databases are averaged (as a function of t_a in this study). The normalized ratios of all NR-PM_1 species positively increased as a function of t_a with different increase rates. At low t_a levels (< 15 h), relatively small ratios of all species could be observed, and all ratios showed a slight increase trend. However, at t_a = 20-30 h, the normalized concentration of total NR-PM_1, OA, SO_4^{2-}, and NH_4^+ increased by a factor of > 5 compared with that at low t_a levels (< 15 h). This indicated that these species were susceptible to

https://doi.org/10.5194/acp-2020-792
Preprint. Discussion started: 25 August 2020


Atmospheric Chemistry and Physics Discussions

photochemical aging processes in the summer, with strong solar radiation. Exponential fitting (y = A×exp(x/B) + C) was applied to quantitatively describe the relationship between these species and t_a, as given in Fig. 3. The fitting parameter B could be used to characterize the sensitivity of each species to the increase of t_a, while smaller B means more sensitivity to t_a. According to the fitting results, the formation of NR-PM_1 was most sensitive to t_a, followed by SO_4^{2-}, OA, and NH_4^+ in sequence. Their average increase rates in absolute mass concentration (Fig. S7) showed the same trend as the normalized ratios in Fig. 3. The average increase rate of SO_4^{2-} was the largest (0.4 μg m^{-3} per hour) among NR-PM_1 species, while that of NR-PM_1 was 0.8 μg m^{-3} per hour. These results also suggested that the photochemical aging process plays an important role in SO_4^{2-} formation in summertime (Li et al., 2020). Previous studies have revealed that an aqueous-phase process plays an important role in SO_4^{2-} formation (Sun et al., 2015; Sun et al., 2013a). However, it appears that photochemical oxidation was the primary pathway of SO_4^{2-} formation in the present summertime observation, as seen in the t_a- and RH-dependent distributions of SO_4^{2-} (Fig. S8). Both the SO_4^{2-} mass concentration and its proportion in PM_1 were highly dependent on t_a rather than RH. The similar evolution trends of NH_4^+ and SO_4^{2-} suggested that NH_4^+ mainly existed in the form of $(NH_4)_2SO_4$ (apart from NH_4NO_3 and NH_4Cl), which could be supported by the relative contributions of these SIA species during this field observation (see Section 3.1). The formation of Cl^- was also boosted with increasing t_a, similar to that of NH_4^+, which confirmed the combination Cl^- with NH_4^+ in the form of NH_4Cl (Chen et al., 2020). As for NO_3^-, the corresponding ratio first increased and then slightly decreased as t_a increased, which was similar to the evolution trend of absolute mass concentration (Fig. S7). It was worth noting that the concentration of NO_x decreased with increasing t_a (Fig. S6), suggesting the photochemical oxidation of NO_x to HNO_3 or NO_3^-. This was in agreement

https://doi.org/10.5194/acp-2020-792
Preprint. Discussion started: 25 August 2020

Atmospheric Chemistry and Physics Discussions

304 with the observation of high concentrations of NO_z ($NO_z = NO_y - NO_x$) at elevated t_a levels (Fig.
305 S6). Meanwhile, high temperature accompanied high levels of t_a (Fig. S6), which could cause the
306 evaporation of NO_3^- or adsorbed HNO_3 into the gas phase (Xu et al., 2019a). As demonstrated by
307 the t_a- and RH-dependent distributions of NO_3^- (Fig. S8), the aqueous-phase process made a
308 significant contribution to the formation of NO_3^- (Duan et al., 2020).

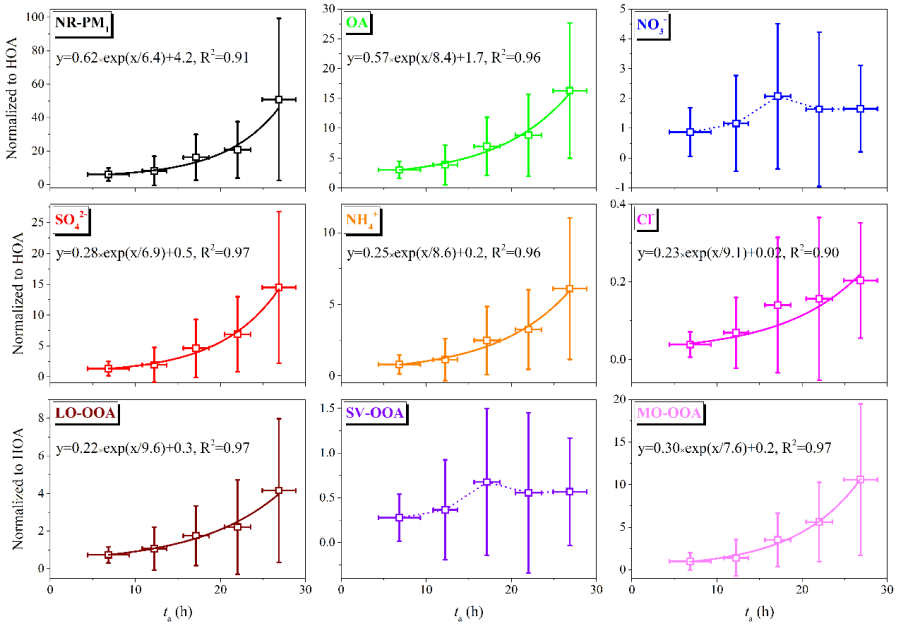

309

310 Figure 3. Variations of the ratios of mass concentrations of NR-PM_1 species and OA factors to HOA
311 as a function of t_a. The data are binned according to the value of t_a (5 h increment). The solid lines
312 are the results of exponential fitting with the function of $y = A \times \exp(x/B) + C$.

313 Regarding the OA factors, they exhibited different dependence on t_a as presented in Fig. 3.
314 Among these four OA factors, MO-OOA was most affected by the increase in t_a, with a factor of
315 ~10 compared with that at low t_a levels (<15 h). The enhancement factor of LO-OOA with increased
316 t_a was ~6, which might be due to its lower oxidation state (OSc = -0.34) than that of MO-OOA (OSc
317 = -0.23). These results are consistent with the exponential fitting parameter B of MO-OOA and LO-

https://doi.org/10.5194/acp-2020-792
Preprint. Discussion started: 25 August 2020

Atmospheric Chemistry and Physics Discussions

OOA in Fig. 3. The average increase rate of MO-OOA (0.3 μg m^{-3} per hour) was also significantly larger than that of LO-OOA, with a factor of ~7. As for SV-OOA, t_a exhibited a slight enhancement effect, suggesting that photochemical aging may be not its main formation pathway. In contrast, the normalized concentration of SV-OOA and its contribution to PM_1 significantly depended on RH (Fig. S9), which was consistent with the results of Herrmann et al. (2015).

Figure 4 shows the averaged contributions of NR-PM_1 species and OA factors at low and high t_a levels. The average mass concentration of NR-PM_1 at t_a >15 h was 22.5 μg m^{-3}, which was 1.4 times of that at t_a <15 h. All NR-PM_1 species were enhanced in mass concentration by a factor of more than 1.1 at elevated t_a, of which SO_4^{2-} had the largest enhancement factor of 2.1. OA was the dominant species in NR-PM_1 at both t_a levels, although its percentage decreased from 57% to 48% with the increase of t_a. This decreased percentage could be attributed to the significantly decreased contribution of HOA (from 39% to 20%) with the enhancement of t_a, suggesting that the photochemical aging process was not conducive to the accumulation of HOA. Comparing the contribution of other species to NR-PM_1 at low and high t_a levels, it was found that the contribution of NO_3^- presented a decreasing trend (from 12% to 10%) as t_a increased, which could be attributed to the lower concentration of NO_x, higher temperature and lower RH, as mentioned above. The contribution of Cl^- did not change with t_a level. The contributions of SO_4^{2-} and NH_4^+ were enhanced from 19% to 27% and 11% to 14%, respectively as t_a increased from 9.4 h to 19.6 h, which confirmed that the formation of SO_4^{2-} greatly benefited from the photochemical process, and that NH_4^+ mainly existed in the form of $(NH_4)_2SO_4$ during this summertime observation.

The OA factors also presented different change trends and different compositions at high t_a levels compared with those at low t_a levels. The OOA accounted for more than half of OA, and

https://doi.org/10.5194/acp-2020-792
Preprint. Discussion started: 25 August 2020

Atmospheric Chemistry and Physics Discussions

showed much higher contribution at high t_a levels than at low t_a levels (61% vs. 80%). Among them, MO-OOA showed the largest enhancement, by a factor of 2.0 from 2.6 to 5.2 μg m^{-3} in absolute mass concentration, and a factor of 1.8 from 27% to 48% in relative contribution, indicating the importance of MO-OOA in PM_1 pollution at elevated t_a during the summertime. The contributions of LO-OOA and SV-OOA were almost equal (~24% and ~8%, respectively) between low and high t_a levels, while the absolute mass concentrations were enhanced by a factor of >1.1 at high t_a levels. On the contrary, the absolute mass concentration of HOA decreased from 3.3 to 1.8 μg m^{-3} during high t_a periods, indicating a negative effect of t_a on the accumulation of HOA.

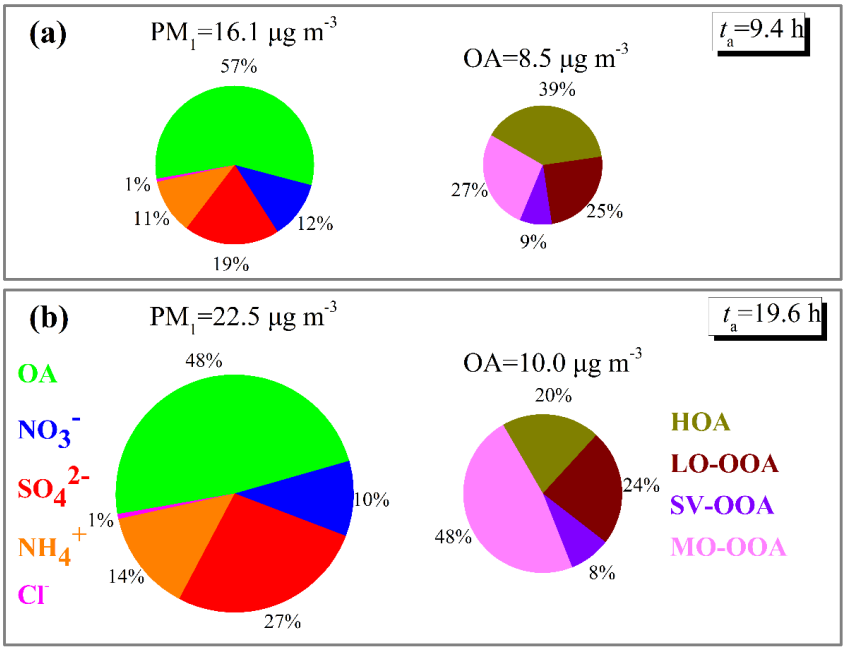

Figure 4. Different chemical compositions of NR-PM_1 and OA factor contributions during the (a) low t_a (< 15 h) period, and (b) high t_a (> 15 h) period. The displayed PM_1, OA, and t_a are averages of values during the corresponding period.

https://doi.org/10.5194/acp-2020-792
Preprint. Discussion started: 25 August 2020

Atmospheric Chemistry and Physics Discussions

3.3 Role of t_a in OA evolution

The role of t_a in the evolution of OA during the summertime was further examined. Fig. 5 shows the variations of H/C, O/C, N/C, S/C, OM/OC, and OSc as a function of t_a. All these parameters except H/C increased with the increase of t_a. The decrease of H/C was related to the decreased contribution of HOA (Fig. 4), since HOA had the highest H/C among these four OA factors (Fig. S1). In contrast to H/C, O/C and OM/OC increased from 0.53 to 0.73 and 1.88 to 2.14 with the increase of t_a, respectively. Moreover, a high correlation coefficient between OM/OC and O/C was observed (R^2 = 0.997, Fig. S10, in the Supplement). These results suggest that OA was highly oxidized due to the progress of atmospheric photochemical aging. Meanwhile, the analogous variation between OSc and O/C confirmed the high oxidation state of OA, since both are metrics of the oxidation degree of OA (Kroll et al., 2011). As for the variation of N/C and S/C, they presented a slight increase trend with the increase in t_a. This indicated that photochemical processes could contribute to the formation of N-containing and S-containing organics, which is consistent with previous smog chamber simulations in the laboratory (Chen et al., 2019c,d).

https://doi.org/10.5194/acp-2020-792
Preprint. Discussion started: 25 August 2020

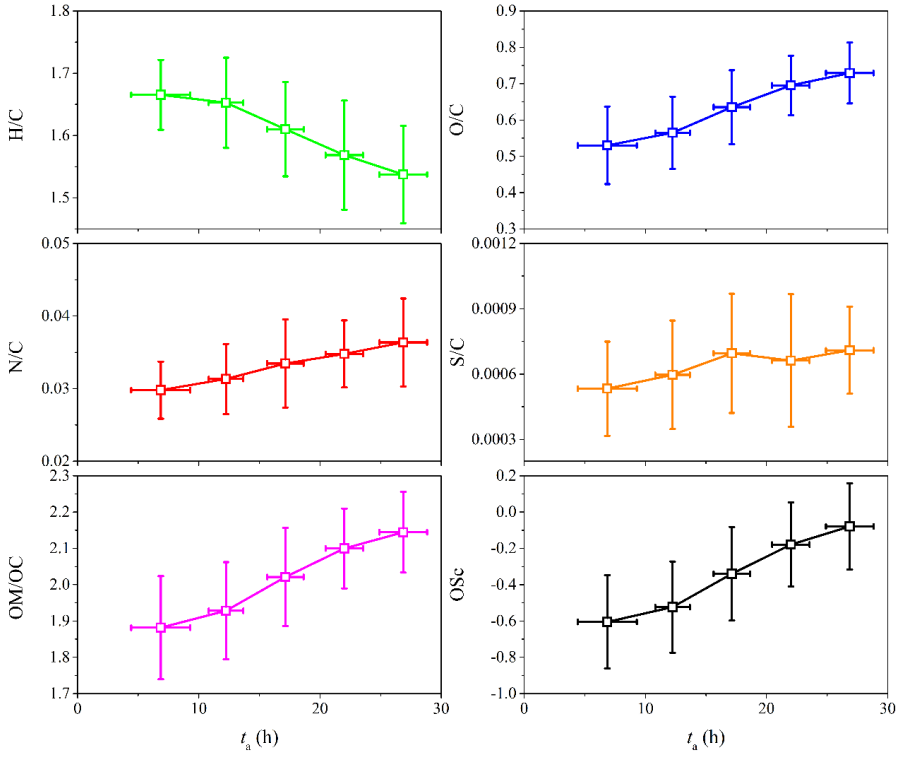

Figure 5. Variations of H/C, O/C, N/C, S/C, OM/OC and OSc as a function of t_a. The data are binned according to the value of t_a (5 h increment).

The binned H/C and O/C as a function of t_a are given in Fig. 6. The fitted slope of -0.63 is similar to those reported in both field observations and laboratory simulations on the photochemical aging of anthropogenic primary OA or biomass burning OA (Chen et al., 2015). This slope can be obtained by a combination of the simultaneous addition of both alcohol (slope = 0) and carbonyl (slope = -2) functional groups, or the addition of carboxylic acid with (slope = -0.5) and without (slope = -1) fragmentation (Peng et al., 2016; Chen et al., 2015; Ng et al., 2011; Heald et al., 2010). Additionally, as t_a increased, the OA evolved from the left top region to the right bottom region of the Van Krevelen diagram, accompanied by a decrease in H/C and increase in O/C. This further indicated that the evolution process of OA was from less oxidized to more aged as the atmospheric

https://doi.org/10.5194/acp-2020-792
Preprint. Discussion started: 25 August 2020

Atmospheric Chemistry and Physics Discussions

photochemical aging progressed, leading to higher PM_1 concentrations.

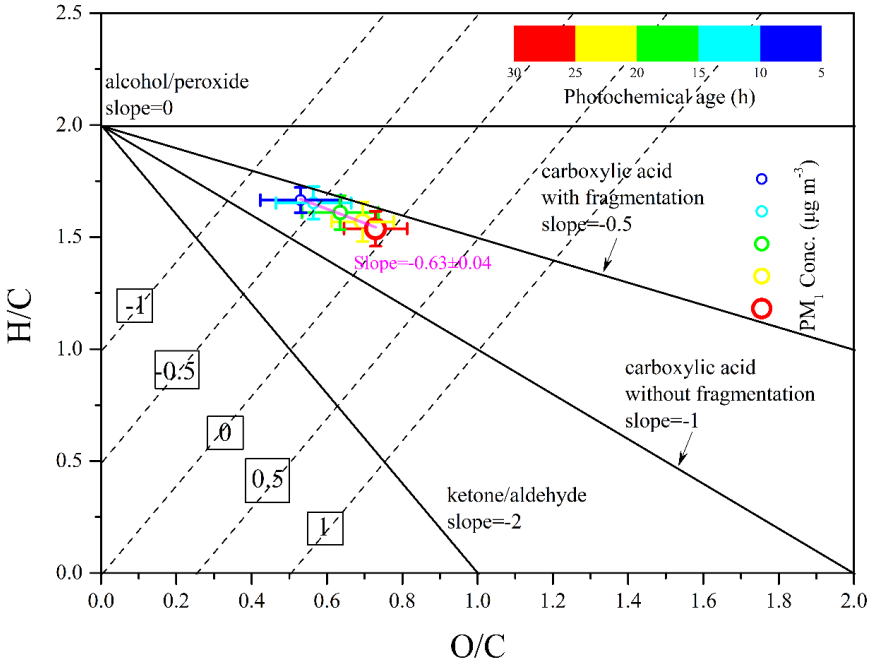

Figure 6. Van Krevelen diagram during this field observation. The data are binned according to the value of t_a (5 h increment) and color coded by t_a. The elemental composition of OA was fitted with a slope of -0.63 (R^2 = 0.98).

4 Conclusions

In this study, a summertime field observation mainly based on the Aerodyne HR-ToF-AMS was carried out to characterize NR-PM_1 in a southern suburb of Beijing from 25th July to 21st August 2019. The role of photochemical age (t_a) in aerosol formation and composition was analyzed. During this period, the averaged NR-PM_1 concentration was 19.3 ± 11.3 μg m^{-3}; of NR-PM_1, OA was the dominant species (48-57%), followed by SO_4^{2-} (19-27%), NO_3^- (10-12%) at different t_a levels. Higher PM_1 concentrations were observed at longer t_a. Meanwhile, with the increase of t_a, the normalized ratios of NR-PM_1 species and OA factors to HOA were greatly enhanced by a factor

https://doi.org/10.5194/acp-2020-792
Preprint. Discussion started: 25 August 2020


Atmospheric Chemistry and Physics Discussions

of >5, especially for OA, SO_4^{2-}, and MO-OOA. The total NR-PM_1 presented the largest average increase rate of 0.8 μg m^{-3} per hour, followed by SO_4^{2-} (0.4 μg m^{-3} per hour) and MO-OOA (0.3 μg m^{-3} per hour). As t_a increased from 9.4 h to 19.6 h, the relative contribution of MO-OOA presented the most obvious promotion from 27% to 48%, suggesting the significance of more-oxidized OA, which mainly originates from the photo-oxidation of VOCs, in PM_1 pollution during the summertime with strong solar radiation. The evolution of OA was also greatly affected by t_a, decreased H/C and increased O/C could be found as t_a increased, along with the larger OSc and OM/OC, indicating that OA went from less oxidized to more aged with the progression of atmospheric photochemical aging, further leading to the higher PM_1 concentration. Our results suggested that the atmospheric photochemical aging process is a crucial factor resulting in the PM_1 pollution in summertime, especially for the formation and evolution of SOA. Previous studies have indicated that NO_x is a highly active species and has a great effect on the source of the main oxidants (e.g., OH, O_3, and NO_3) (Seinfeld and Pandis, 2016). Therefore, NO_x and VOCs, mainly from vehicle-related emissions (Liu et al., 2019a; Qin et al., 2017), should be strictly controlled to lower the atmospheric oxidation capacity characterized by OH exposure dose to further ease the PM pollution in summertime.

Considering there would be differences in the formation and evolution of PM_1 between different seasons, and few field observations have been conducted in suburban areas of Beijing, further works should be carried out to shed light on the seasonal variations of PM_1 and their formation and evolution mechanisms in different seasons in suburban areas. Additionally, the detailed role of photochemical age (t_a) in the formation of the secondary gaseous pollutant O_3, as well as their relationship in different seasons, should also be of concern because O_3 has become the

https://doi.org/10.5194/acp-2020-792
Preprint. Discussion started: 25 August 2020


Atmospheric Chemistry and Physics Discussions

primary air pollutant, especially in summertime.

Declarations of interest

The authors declare that they have no conflict of interest.

Acknowledgements

The authors are grateful to all workers for their support during this filed observation. The authors acknowledge the National Natural Science Foundation of China (21922610, 21876185, 91744205, and 41877304), the Youth Innovation Promotion Association, CAS (2018055, 2018060, and 2017064), and the Young Talent Project of the Center for Excellence in Regional Atmospheric Environment, CAS (CERAE201801). The authors would also like to thank Ms. Qingcai Feng for her help editing this paper.

Supplement

Supplementary data to this article can be found online.

Author contributions

HH, YM, YL, and QM designed this filed observation. TC, JL, and QM conducted the measurements and data analyses. TC, JL, QM, BC, PZ, CZ, and YL interpreted and discussed the data results. TC wrote the paper with input from all coauthors. All authors contributed to the final paper.

References

An, Z., Huang, R.-J., Zhang, R., Tie, X., Li, G., Cao, J., Zhou, W., Shi, Z., Han, Y., Gu, Z., and Ji, Y.: Severe haze in northern China: A synergy of anthropogenic emissions and atmospheric processes, Proc. Natl. Acad. Sci. USA, 116, 8657-8666, 10.1073/pnas.1900125116, 2019.

Atkinson, R., and Arey, J.: Atmospheric degradation of volatile organic compounds, Chem. Rev., 103,

https://doi.org/10.5194/acp-2020-792
Preprint. Discussion started: 25 August 2020

435 4605-4638, 10.1021/cr0206420, 2003.

436 Canagaratna, M. R., Jimenez, J. L., Kroll, J. H., Chen, Q., Kessler, S. H., Massoli, P., Hildebrandt Ruiz,
437 L., Fortner, E., Williams, L. R., Wilson, K. R., Surratt, J. D., Donahue, N. M., Jayne, J. T., and Worsnop,
438 D. R.: Elemental ratio measurements of organic compounds using aerosol mass spectrometry:
439 characterization, improved calibration, and implications, Atmos. Chem. Phys., 15, 253-272,
440 10.5194/acp-15-253-2015, 2015.

441 Chen, Q., Heald, C. L., Jimenez, J. L., Canagaratna, M. R., Zhang, Q., He, L.-Y., Huang, X.-F.,
442 Campuzano-Jost, P., Palm, B. B., Poulain, L., Kuwata, M., Martin, S. T., Abbatt, J. P. D., Lee, A. K. Y.,
443 and Liggio, J.: Elemental composition of organic aerosol: The gap between ambient and laboratory
444 measurements, Geophys. Res. Lett., 42, 4182-4189, 10.1002/2015gl063693, 2015.

445 Chen, T., Chu, B., Ge, Y., Zhang, S., Ma, Q., He, H., and Li, S.-M.: Enhancement of aqueous sulfate
446 formation by the coexistence of NO_2/NH_3 under high ionic strengths in aerosol water, Environ. Pollut.,
447 252, 236-244, https://doi.org/10.1016/j.envpol.2019.05.119, 2019a.

448 Chen, T., Liu, Y., Chu, B., Liu, C., Liu, J., Ge, Y., Ma, Q., Ma, J., and He, H.: Differences of the oxidation
449 process and secondary organic aerosol formation at low and high precursor concentrations, J. Environ.
450 Sci., 79, 256-263, 10.1016/j.jes.2018.11.011, 2019b.

451 Chen, T., Liu, Y., Liu, C., Liu, J., Chu, B., and He, H.: Important role of aromatic hydrocarbons in SOA
452 formation from unburned gasoline vapor, Atmos. Environ., 201, 101-109,
453 10.1016/j.atmosenv.2019.01.001, 2019c.

454 Chen, T., Liu, Y., Ma, Q., Chu, B., Zhang, P., Liu, C., Liu, J., and He, H.: Significant source of secondary
455 aerosol: Formation from gasoline evaporative emissions in the presence of SO_2 and NH_3, Atmos. Chem.
456 Phys., 19, 8063-8081, 10.5194/acp-19-8063-2019, 2019d.

https://doi.org/10.5194/acp-2020-792
Preprint. Discussion started: 25 August 2020

457 Chen, T., Liu, J., Liu, Y., Ma, Q., Ge, Y., Zhong, C., Jiang, H., Chu, B., Zhang, P., Ma, J., Liu, P., Wang,
458 Y., Mu, Y., and He, H.: Chemical characterization of submicron aerosol in summertime Beijing: A case
459 study in southern suburbs in 2018, Chemosphere, 247, 125918,
460 https://doi.org/10.1016/j.chemosphere.2020.125918, 2020.
461 Cheng, Y., Zheng, G., Wei, C., Mu, Q., Zheng, B., Wang, Z., Gao, M., Zhang, Q., He, K., Carmichael,
462 G., Pöschl, U., and Su, H.: Reactive nitrogen chemistry in aerosol water as a source of sulfate during
463 haze events in China, Sci. Adv., 2, e1601530, 10.1126/sciadv.1601530, 2016.
464 Davidson, C. I., Phalen, R. F., and Solomon, P. A.: Airborne particulate matter and human health: a review,
465 Aerosol Sci. Tech., 39, 737-749, 10.1080/02786820500191348, 2005.
466 de Gouw, J. A., Middlebrook, A. M., Warneke, C., Goldan, P. D., Kuster, W. C., Roberts, J. M., Fehsenfeld,
467 F. C., Worsnop, D. R., Canagaratna, M. R., Pszenny, A. A. P., Keene, W. C., Marchewka, M., Bertman,
468 S. B., and Bates, T. S.: Budget of organic carbon in a polluted atmosphere: Results from the New England
469 Air Quality Study in 2002, J. Geophys. Res., 110, 10.1029/2004jd005623, 2005.
470 DeCarlo, P. F., Kimmel, J. R., Trimborn, A., Northway, M. J., Jayne, J. T., Aiken, A. C., Gonin, M., Fuhrer,
471 K., Horvath, T., Docherty, K. S., Worsnop, D. R., and Jimenez, J. L.: Field-deployable, high-resolution,
472 time-of-flight aerosol mass spectrometer, Anal. Chem., 78, 8281-8289, 10.1021/ac061249n, 2006.
473 Drewnick, F., Hings, S. S., DeCarlo, P., Jayne, J. T., Gonin, M., Fuhrer, K., Weimer, S., Jimenez, J. L.,
474 Demerjian, K. L., Borrmann, S., and Worsnop, D. R.: A new time-of-flight aerosol mass spectrometer
475 (TOF-AMS)—instrument description and first field deployment, Aerosol Sci. Tech., 39, 637-658,
476 10.1080/02786820500182040, 2005.
477 Duan, J., Huang, R. J., Lin, C., Dai, W., Wang, M., Gu, Y., Wang, Y., Zhong, H., Zheng, Y., Ni, H., Dusek,
478 U., Chen, Y., Li, Y., Chen, Q., Worsnop, D. R., O'Dowd, C. D., and Cao, J.: Distinctions in source regions

https://doi.org/10.5194/acp-2020-792
Preprint. Discussion started: 25 August 2020


Atmospheric Chemistry and Physics Discussions

479 and formation mechanisms of secondary aerosol in Beijing from summer to winter, Atmos. Chem. Phys.,
480 19, 10319-10334, 10.5194/acp-19-10319-2019, 2019.
481 Duan, J., Huang, R. J., Li, Y., Chen, Q., Zheng, Y., Chen, Y., Lin, C., Ni, H., Wang, M., Ovadnevaite, J.,
482 Ceburnis, D., Chen, C., Worsnop, D. R., Hoffmann, T., O'Dowd, C., and Cao, J.: Summertime and
483 wintertime atmospheric processes of secondary aerosol in Beijing, Atmos. Chem. Phys., 20, 3793-3807,
484 10.5194/acp-20-3793-2020, 2020.
485 Elser, M., Huang, R. J., Wolf, R., Slowik, J. G., Wang, Q., Canonaco, F., Li, G., Bozzetti, C., Daellenbach,
486 K. R., Huang, Y., Zhang, R., Li, Z., Cao, J., Baltensperger, U., El-Haddad, I., and Prévôt, A. S. H.: New
487 insights into $PM_{2.5}$ chemical composition and sources in two major cities in China during extreme haze
488 events using aerosol mass spectrometry, Atmos. Chem. Phys., 16, 3207-3225, 10.5194/acp-16-3207-
489 2016, 2016.
490 Fan, Y., Liu, C. Q., Li, L., Ren, L., Ren, H., Zhang, Z., Li, Q., Wang, S., Hu, W., Deng, J., Wu, L., Zhong,
491 S., Zhao, Y., Pavuluri, C. M., Li, X., Pan, X., Sun, Y., Wang, Z., Kawamura, K., Shi, Z., and Fu, P.: Large
492 contributions of biogenic and anthropogenic sources to fine organic aerosols in Tianjin, North China,
493 Atmos. Chem. Phys., 20, 117-137, 10.5194/acp-20-117-2020, 2020.
494 Feng, T., Zhao, S., Bei, N., Wu, J., Liu, S., Li, X., Liu, L., Qian, Y., Yang, Q., Wang, Y., Zhou, W., Cao,
495 J., and Li, G.: Secondary organic aerosol enhanced by increasing atmospheric oxidizing capacity in
496 Beijing–Tianjin–Hebei (BTH), China, Atmos. Chem. Phys., 19, 7429-7443, 10.5194/acp-19-7429-2019,
497 2019.
498 Fu, P., Kawamura, K., Kanaya, Y., and Wang, Z.: Contributions of biogenic volatile organic compounds
499 to the formation of secondary organic aerosols over Mt. Tai, Central East China, Atmos. Environ., 44,
500 4817-4826, https://doi.org/10.1016/j.atmosenv.2010.08.040, 2010.

https://doi.org/10.5194/acp-2020-792
Preprint. Discussion started: 25 August 2020

Atmospheric Chemistry and Physics Discussions

501 Fu, P., Kawamura, K., Chen, J., and Miyazaki, Y.: Secondary Production of Organic Aerosols from
502 Biogenic VOCs over Mt. Fuji, Japan, Environ. Sci. Technol., 48, 8491-8497, 10.1021/es500794d, 2014.
503 Garmash, O., Rissanen, M. P., Pullinen, I., Schmitt, S., Kausiala, O., Tillmann, R., Zhao, D., Percival, C.,
504 Bannan, T. J., Priestley, M., Hallquist, Å. M., Kleist, E., Kiendler-Scharr, A., Hallquist, M., Berndt, T.,
505 McFiggans, G., Wildt, J., Mentel, T. F., and Ehn, M.: Multi-generation OH oxidation as a source for
506 highly oxygenated organic molecules from aromatics, Atmos. Chem. Phys., 20, 515-537, 10.5194/acp-
507 20-515-2020, 2020.
508 Ge, X., Li, L., Chen, Y., Chen, H., Wu, D., Wang, J., Xie, X., Ge, S., Ye, Z., Xu, J., and Chen, M.: Aerosol
509 characteristics and sources in Yangzhou, China resolved by offline aerosol mass spectrometry and other
510 techniques, Environ. Pollut., 225, 74-85, 10.1016/j.envpol.2017.03.044, 2017.
511 Gelencsér, A., Siszler, K., and Hlavay, J.: Toluene−Benzene Concentration Ratio as a Tool for
512 Characterizing the Distance from Vehicular Emission Sources, Environ. Sci. Technol., 31, 2869-2872,
513 10.1021/es970004c, 1997.
514 Guo, S., Hu, M., Zamora, M. L., Peng, J., Shang, D., Zheng, J., Du, Z., Wu, Z., Shao, M., Zeng, L.,
515 Molina, M. J., and Zhang, R.: Elucidating severe urban haze formation in China, Proc. Natl. Acad. Sci.
516 USA, 111, 17373-17378, 10.1073/pnas.1419604111, 2014.
517 Hallquist, M., Wenger, J. C., Baltensperger, U., Rudich, Y., Simpson, D., Claeys, M., Dommen, J.,
518 Donahue, N. M., George, C., Goldstein, A. H., Hamilton, J. F., Herrmann, H., Hoffmann, T., Iinuma, Y.,
519 Jang, M., Jenkin, M. E., Jimenez, J. L., Kiendler-Scharr, A., Maenhaut, W., McFiggans, G., Mentel, T.
520 F., Monod, A., Prévôt, A. S. H., Seinfeld, J. H., Surratt, J. D., Szmigielski, R., and Wildt, J.: The formation,
521 properties and impact of secondary organic aerosol: current and emerging issues, Atmos. Chem. Phys.,
522 9, 5155-5236, 10.5194/acp-9-5155-2009, 2009.

https://doi.org/10.5194/acp-2020-792
Preprint. Discussion started: 25 August 2020

523 Heald, C. L., Kroll, J. H., Jimenez, J. L., Docherty, K. S., DeCarlo, P. F., Aiken, A. C., Chen, Q., Martin,
524 S. T., Farmer, D. K., and Artaxo, P.: A simplified description of the evolution of organic aerosol
525 composition in the atmosphere, Geophys. Res. Lett., 37, L08803, 10.1029/2010GL042737, 2010.
526 Herrmann, H., Schaefer, T., Tilgner, A., Styler, S. A., Weller, C., Teich, M., and Otto, T.: Tropospheric
527 aqueous-phase chemistry: kinetics, mechanisms, and its coupling to a changing gas phase, Chem. Rev.,
528 115, 4259-4334, 10.1021/cr500447k, 2015.
529 Hu, W., Hu, M., Hu, W., Jimenez, J. L., Yuan, B., Chen, W., Wang, M., Wu, Y., Chen, C., Wang, Z., Peng,
530 J., Zeng, L., and Shao, M.: Chemical composition, sources, and aging process of submicron aerosols in
531 Beijing: Contrast between summer and winter, J. Geophys. Res. Atmos., 121, 1955-1977,
532 doi:10.1002/2015JD024020, 2016.
533 Hu, W., Hu, M., Hu, W. W., Zheng, J., Chen, C., Wu, Y., and Guo, S.: Seasonal variations in high time-
534 resolved chemical compositions, sources, and evolution of atmospheric submicron aerosols in the
535 megacity Beijing, Atmos. Chem. Phys., 17, 9979-10000, 10.5194/acp-17-9979-2017, 2017.
536 Hua, Y., Wang, S., Jiang, J., Zhou, W., Xu, Q., Li, X., Liu, B., Zhang, D., and Zheng, M.: Characteristics
537 and sources of aerosol pollution at a polluted rural site southwest in Beijing, China, Sci. Total Environ.,
538 626, 519-527, 10.1016/j.scitotenv.2018.01.047, 2018.
539 Huang, D. D., Li, Y. J., Lee, B. P., and Chan, C. K.: Analysis of organic sulfur compounds in atmospheric
540 aerosols at the HKUST supersite in Hong Kong using HR-ToF-AMS, Environ. Sci. Technol., 49, 3672-
541 3679, 10.1021/es5056269, 2015.
542 Huang, R.-J., Zhang, Y., Bozzetti, C., Ho, K.-F., Cao, J.-J., Han, Y., Daellenbach, K. R., Slowik, J. G.,
543 Platt, S. M., Canonaco, F., Zotter, P., Wolf, R., Pieber, S. M., Bruns, E. A., Crippa, M., Ciarelli, G.,
544 Piazzalunga, A., Schwikowski, M., Abbaszade, G., Schnelle-Kreis, J., Zimmermann, R., An, Z., Szidat,

https://doi.org/10.5194/acp-2020-792
Preprint. Discussion started: 25 August 2020

Atmospheric Chemistry and Physics Discussions

545 S., Baltensperger, U., Haddad, I. E., and Prevot, A. S. H.: High secondary aerosol contribution to
546 particulate pollution during haze events in China, Nature, 514, 218-222, 10.1038/nature13774, 2014.
547 Huang, R. J., Wang, Y., Cao, J., Lin, C., Duan, J., Chen, Q., Li, Y., Gu, Y., Yan, J., Xu, W., Fröhlich, R.,
548 Canonaco, F., Bozzetti, C., Ovadnevaite, J., Ceburnis, D., Canagaratna, M. R., Jayne, J., Worsnop, D. R.,
549 El-Haddad, I., Prévôt, A. S. H., and O'Dowd, C. D.: Primary emissions versus secondary formation of
550 fine particulate matter in the most polluted city (Shijiazhuang) in North China, Atmos. Chem. Phys., 19,
551 2283-2298, 10.5194/acp-19-2283-2019, 2019.
552 Huang, X. F., He, L. Y., Hu, M., Canagaratna, M. R., Sun, Y., Zhang, Q., Zhu, T., Xue, L., Zeng, L. W.,
553 Liu, X. G., Zhang, Y. H., Jayne, J. T., Ng, N. L., and Worsnop, D. R.: Highly time-resolved chemical
554 characterization of atmospheric submicron particles during 2008 Beijing Olympic Games using an
555 Aerodyne High-Resolution Aerosol Mass Spectrometer, Atmos. Chem. Phys., 10, 8933-8945,
556 10.5194/acp-10-8933-2010, 2010.
557 IPCC: Climate Change 2013: The Physical Science Basis. Contribution of Working Group I to the Fifth
558 Assessment Report of the Intergovernmental Panel on Climate Change, Cambridge University Press,
559 Cambridge, United Kingdom and New York, NY, USA, 1535 pp., 2013.
560 Jimenez, J. L., Jayne, J. T., Shi, Q., Kolb, C. E., Worsnop, D. R., Yourshaw, I., Seinfeld, J. H., Flagan, R.
561 C., Zhang, X., Smith, K. A., Morris, J. W., and Davidovits, P.: Ambient aerosol sampling using the
562 aerodyne aerosol mass spectrometer, J. Geophys. Res. Atmos., 108, 8425, 10.1029/2001JD001213, 2003.
563 Kroll, J. H., Donahue, N. M., Jimenez, J. L., Kessler, S. H., Canagaratna, M. R., Wilson, K. R., Altieri,
564 K. E., Mazzoleni, L. R., Wozniak, A. S., Bluhm, H., Mysak, E. R., Smith, J. D., Kolb, C. E., and Worsnop,
565 D. R.: Carbon oxidation state as a metric for describing the chemistry of atmospheric organic aerosol,
566 Nat. Chem., 3, 133-139, 10.1038/nchem.948, 2011.

https://doi.org/10.5194/acp-2020-792
Preprint. Discussion started: 25 August 2020

Atmospheric Chemistry and Physics Discussions

Li, J., Liu, Q., Li, Y., Liu, T., Huang, D., Zheng, J., Zhu, W., Hu, M., Wu, Y., Lou, S., Hallquist, A. M., Hallquist, M., Chan, C. K., Canonaco, F., Prevot, A. S. H., Fung, J. C. H., Lau, A. K. H., and Yu, J. Z.: Characterization of Aerosol Aging Potentials at Suburban Sites in Northern and Southern China Utilizing a Potential Aerosol Mass (Go:PAM) Reactor and an Aerosol Mass Spectrometer, J. Geophys. Res. Atmos., 124, 5629-5649, 10.1029/2018jd029904, 2019a.

Li, J., Cao, L., Gao, W., He, L., Yan, Y., Ji, D., Liu, Z., and Wang, Y.: Seasonal variations in the high time-resolved aerosol composition, sources, and chemical process of background submicron particles in North China Plain, Atmos. Chem. Phys. Discuss., 2020, 1-26, 10.5194/acp-2020-213, 2020.

Li, K., Jacob, D. J., Liao, H., Shen, L., Zhang, Q., and Bates, K. H.: Anthropogenic drivers of 2013-2017 trends in summer surface ozone in China, Proc. Natl. Acad. Sci. USA, 116, 422-427, 10.1073/pnas.1812168116, 2019b.

Li, K., Jacob, D. J., Liao, H., Zhu, J., Shah, V., Shen, L., Bates, K. H., Zhang, Q., and Zhai, S.: A two-pollutant strategy for improving ozone and particulate air quality in China, Nat. Geosci., 12, 906-910, 10.1038/s41561-019-0464-x, 2019c.

Li, L., Ren, L., Ren, H., Yue, S., Xie, Q., Zhao, W., Kang, M., Li, J., Wang, Z., Sun, Y., and Fu, P.: Molecular Characterization and Seasonal Variation in Primary and Secondary Organic Aerosols in Beijing, China, J. Geophys. Res. Atmos., 123, 12,394-312,412, 10.1029/2018jd028527, 2018a.

Li, Q., Zhang, L., Wang, T., Wang, Z., Fu, X., and Zhang, Q.: "New" Reactive Nitrogen Chemistry Reshapes the Relationship of Ozone to Its Precursors, Environ. Sci. Technol., 52, 2810-2818, 10.1021/acs.est.7b05771, 2018b.

Li, Y. J., Lee, B. Y. L., Yu, J. Z., Ng, N. L., and Chan, C. K.: Evaluating the degree of oxygenation of organic aerosol during foggy and hazy days in Hong Kong using high-resolution time-of-flight aerosol

https://doi.org/10.5194/acp-2020-792
Preprint. Discussion started: 25 August 2020

Atmospheric Chemistry and Physics Discussions

589 mass spectrometry (HR-ToF-AMS), Atmos. Chem. Phys., 13, 8739-8753, 10.5194/acp-13-8739-2013,
590 2013.
591 Li, Y. J., Lee, B. P., Su, L., Fung, J. C. H., and Chan, C. K.: Seasonal characteristics of fine particulate
592 matter (PM) based on high-resolution time-of-flight aerosol mass spectrometric (HR-ToF-AMS)
593 measurements at the HKUST Supersite in Hong Kong, Atmos. Chem. Phys., 15, 37-53, 10.5194/acp-15-
594 37-2015, 2015.
595 Li, Y. J., Sun, Y., Zhang, Q., Li, X., Li, M., Zhou, Z., and Chan, C. K.: Real-time chemical
596 characterization of atmospheric particulate matter in China: A review, Atmos. Environ., 158, 270-304,
597 https://doi.org/10.1016/j.atmosenv.2017.02.027, 2017.
598 Liu, H., Qi, L., Liang, C., Deng, F., Man, H., and He, K.: How aging process changes characteristics of
599 vehicle emissions? A review, Crit. Rev. Environ. Sci. Technol., 10.1080/10643389.2019.1669402, 2019a.
600 Liu, M., Huang, X., Song, Y., Tang, J., Cao, J., Zhang, X., Zhang, Q., Wang, S., Xu, T., Kang, L., Cai,
601 X., Zhang, H., Yang, F., Wang, H., Yu, J. Z., Lau, A. K. H., He, L., Huang, X., Duan, L., Ding, A., Xue,
602 L., Gao, J., Liu, B., and Zhu, T.: Ammonia emission control in China would mitigate haze pollution and
603 nitrogen deposition, but worsen acid rain, Proc. Natl. Acad. Sci. USA, 116, 7760-7765,
604 10.1073/pnas.1814880116, 2019b.
605 Liu, Q., Sun, Y., Hu, B., Liu, Z., Akio, S., and Wang, Y.: In situ measurement of PM_1 organic aerosol in
606 Beijing winter using a high-resolution aerosol mass spectrometer, Chinese. Sci. Bull., 57, 819-826,
607 10.1007/s11434-011-4886-0, 2012.
608 McKeen, S. A., Liu, S. C., Hsie, E.-Y., Lin, X., Bradshaw, J. D., Smyth, S., Gregory, G. L., and Blake,
609 D. R.: Hydrocarbon ratios during PEM-WEST A: A model perspective, J. Geophys. Res. Atmos., 101,
610 2087-2109, 10.1029/95jd02733, 1996.

https://doi.org/10.5194/acp-2020-792
Preprint. Discussion started: 25 August 2020

Atmospheric Chemistry and Physics Discussions

611 Middlebrook, A. M., Bahreini, R., Jimenez, J. L., and Canagaratna, M. R.: Evaluation of composition-
612 dependent collection efficiencies for the Aerodyne aerosol mass spectrometer using field data, Aerosol
613 Sci. Tech., 46, 258-271, 10.1080/02786826.2011.620041, 2012.
614 Molina, M. J., and Molina, L. T.: Megacities and atmospheric pollution, J. Air Waste Manage., 54, 644-
615 680, 10.1080/10473289.2004.10470936, 2004.
616 Ng, N. L., Canagaratna, M. R., Jimenez, J. L., Chhabra, P. S., Seinfeld, J. H., and Worsnop, D. R.:
617 Changes in organic aerosol composition with aging inferred from aerosol mass spectra, Atmos. Chem.
618 Phys., 11, 6465-6474, 10.5194/acp-11-6465-2011, 2011.
619 Odum, J. R., Hoffmann, T., Bowman, F., Collins, D., Flagan, R. C., and Seinfeld, J. H.: Gas/particle
620 partitioning and secondary organic aerosol yields, Environ. Sci. Technol., 30, 2580-2585,
621 10.1021/es950943+, 1996.
622 Paatero, P., and Tapper, U.: Positive matrix factorization: a non-negative factor model with optimal
623 utilization of error estimates of data values, Environmetrics, 5, 111-126, 10.1002/env.3170050203, 1994.
624 Paatero, P.: Least squares formulation of robust non-negative factor analysis, Chemometr. Intell. Lab, 37,
625 23-35, 10.1016/S0169-7439(96)00044-5, 1997.
626 Parrish, D. D., Stohl, A., Forster, C., Atlas, E. L., Blake, D. R., Goldan, P. D., Kuster, W. C., and de Gouw,
627 J. A.: Effects of mixing on evolution of hydrocarbon ratios in the troposphere, J. Geophys. Res. Atmos.,
628 112, 10.1029/2006jd007583, 2007.
629 Peng, J., Hu, M., Gong, Z., Tian, X., Wang, M., Zheng, J., Guo, Q., Cao, W., Lv, W., Hu, W., Wu, Z., and
630 Guo, S.: Evolution of secondary inorganic and organic aerosols during transport: A case study at a
631 regional receptor site, Environ. Pollut., 218, 794-803, 10.1016/j.envpol.2016.08.003, 2016.
632 Qin, Y. M., Li, Y. J., Wang, H., Lee, B. P. Y. L., Huang, D. D., and Chan, C. K.: Particulate matter (PM)

https://doi.org/10.5194/acp-2020-792
Preprint. Discussion started: 25 August 2020

Atmospheric Chemistry and Physics Discussions

episodes at a suburban site in Hong Kong: evolution of PM characteristics and role of photochemistry in secondary aerosol formation, Atmos. Chem. Phys., 16, 14131-14145, 10.5194/acp-16-14131-2016, 2016.

Qin, Y. M., Tan, H. B., Li, Y. J., Schurman, M. I., Li, F., Canonaco, F., Prévôt, A. S. H., and Chan, C. K.: Impacts of traffic emissions on atmospheric particulate nitrate and organics at a downwind site on the periphery of Guangzhou, China, Atmos. Chem. Phys., 17, 10245-10258, 10.5194/acp-17-10245-2017, 2017.

Schnell, J. L., and Prather, M. J.: Co-occurrence of extremes in surface ozone, particulate matter, and temperature over eastern North America, Proc. Natl. Acad. Sci. USA, 114, 2854-2859, 10.1073/pnas.1614453114, 2017.

Seinfeld, J. H., and Pandis, S. N.: Atmospheric chemistry and physics: from air pollution to climate change, John Wiley & Sons, Hoboken, NJ, 2016.

Shi, Z., Vu, T., Kotthaus, S., Harrison, R. M., Grimmond, S., Yue, S., Zhu, T., Lee, J., Han, Y., Demuzere, M., Dunmore, R. E., Ren, L., Liu, D., Wang, Y., Wild, O., Allan, J., Acton, W. J., Barlow, J., Barratt, B., Beddows, D., Bloss, W. J., Calzolai, G., Carruthers, D., Carslaw, D. C., Chan, Q., Chatzidiakou, L., Chen, Y., Crilley, L., Coe, H., Dai, T., Doherty, R., Duan, F., Fu, P., Ge, B., Ge, M., Guan, D., Hamilton, J. F., He, K., Heal, M., Heard, D., Hewitt, C. N., Hollaway, M., Hu, M., Ji, D., Jiang, X., Jones, R., Kalberer, M., Kelly, F. J., Kramer, L., Langford, B., Lin, C., Lewis, A. C., Li, J., Li, W., Liu, H., Liu, J., Loh, M., Lu, K., Lucarelli, F., Mann, G., McFiggans, G., Miller, M. R., Mills, G., Monk, P., Nemitz, E., O'Connor, F., Ouyang, B., Palmer, P. I., Percival, C., Popoola, O., Reeves, C., Rickard, A. R., Shao, L., Shi, G., Spracklen, D., Stevenson, D., Sun, Y., Sun, Z., Tao, S., Tong, S., Wang, Q., Wang, W., Wang, X., Wang, X., Wang, Z., Wei, L., Whalley, L., Wu, X., Wu, Z., Xie, P., Yang, F., Zhang, Q., Zhang, Y., Zhang, Y., and Zheng, M.: Introduction to the special issue “In-depth study of air pollution sources and processes

https://doi.org/10.5194/acp-2020-792
Preprint. Discussion started: 25 August 2020

Atmospheric Chemistry and Physics Discussions

within Beijing and its surrounding region (APHH-Beijing)", Atmos. Chem. Phys., 19, 7519-7546, 10.5194/acp-19-7519-2019, 2019.

Sun, J., Zhang, Q., Canagaratna, M. R., Zhang, Y., Ng, N. L., Sun, Y., Jayne, J. T., Zhang, X., Zhang, X., and Worsnop, D. R.: Highly time- and size-resolved characterization of submicron aerosol particles in Beijing using an Aerodyne Aerosol Mass Spectrometer, Atmos. Environ., 44, 131-140, 10.1016/j.atmosenv.2009.03.020, 2010.

Sun, P., Nie, W., Chi, X., Xie, Y., Huang, X., Xu, Z., Qi, X., Xu, Z., Wang, L., Wang, T., Zhang, Q., and Ding, A.: Two years of online measurement of fine particulate nitrate in the western Yangtze River Delta: influences of thermodynamics and N_2O_5 hydrolysis, Atmos. Chem. Phys., 18, 17177-17190, 10.5194/acp-18-17177-2018, 2018a.

Sun, Y., Wang, Z., Dong, H., Yang, T., Li, J., Pan, X., Chen, P., and Jayne, J. T.: Characterization of summer organic and inorganic aerosols in Beijing, China with an Aerosol Chemical Speciation Monitor, Atmos. Environ., 51, 250-259, 10.1016/j.atmosenv.2012.01.013, 2012.

Sun, Y., Wang, Z., Fu, P., Jiang, Q., Yang, T., Li, J., and Ge, X.: The impact of relative humidity on aerosol composition and evolution processes during wintertime in Beijing, China, Atmos. Environ., 77, 927-934, https://doi.org/10.1016/j.atmosenv.2013.06.019, 2013a.

Sun, Y., Chen, C., Zhang, Y., Xu, W., Zhou, L., Cheng, X., Zheng, H., Ji, D., Li, J., Tang, X., Fu, P., and Wang, Z.: Rapid formation and evolution of an extreme haze episode in Northern China during winter 2015, Sci. Rep., 6, 27151, 10.1038/srep27151, 2016a.

Sun, Y., Du, W., Fu, P., Wang, Q., Li, J., Ge, X., Zhang, Q., Zhu, C., Ren, L., Xu, W., Zhao, J., Han, T., Worsnop, D. R., and Wang, Z.: Primary and secondary aerosols in Beijing in winter: sources, variations and processes, Atmos. Chem. Phys., 16, 8309-8329, 10.5194/acp-16-8309-2016, 2016b.

https://doi.org/10.5194/acp-2020-792
Preprint. Discussion started: 25 August 2020

677 Sun, Y., Xu, W., Zhang, Q., Jiang, Q., Canonaco, F., Prévôt, A. S. H., Fu, P., Li, J., Jayne, J., Worsnop,
678 D. R., and Wang, Z.: Source apportionment of organic aerosol from 2-year highly time-resolved
679 measurements by an aerosol chemical speciation monitor in Beijing, China, Atmos. Chem. Phys., 18,
680 8469-8489, 10.5194/acp-18-8469-2018, 2018b.
681 Sun, Y. L., Wang, Z. F., Fu, P. Q., Yang, T., Jiang, Q., Dong, H. B., Li, J., and Jia, J. J.: Aerosol
682 composition, sources and processes during wintertime in Beijing, China, Atmos. Chem. Phys., 13, 4577-
683 4592, 10.5194/acp-13-4577-2013, 2013b.
684 Sun, Y. L., Jiang, Q., Wang, Z. F., Fu, P. Q., Li, J., Yang, T., and Yin, Y.: Investigation of the sources and
685 evolution processes of severe haze pollution in Beijing in January 2013, J. Geophys. Res. Atmos., 119,
686 4380-4398, 10.1002/2014jd021641, 2014.
687 Sun, Y. L., Wang, Z. F., Du, W., Zhang, Q., Wang, Q. Q., Fu, P. Q., Pan, X. L., Li, J., Jayne, J., and
688 Worsnop, D. R.: Long-term real-time measurements of aerosol particle composition in Beijing, China:
689 seasonal variations, meteorological effects, and source analysis, Atmos. Chem. Phys., 15, 10149-10165,
690 10.5194/acp-15-10149-2015, 2015.
691 Tan, Z., Lu, K., Jiang, M., Su, R., Wang, H., Lou, S., Fu, Q., Zhai, C., Tan, Q., Yue, D., Chen, D., Wang,
692 Z., Xie, S., Zeng, L., and Zhang, Y.: Daytime atmospheric oxidation capacity in four Chinese megacities
693 during the photochemically polluted season: a case study based on box model simulation, Atmos. Chem.
694 Phys., 19, 3493-3513, 10.5194/acp-19-3493-2019, 2019.
695 Tie, X., Huang, R.-J., Cao, J., Zhang, Q., Cheng, Y., Su, H., Chang, D., Poeschl, U., Hoffmann, T., Dusek,
696 U., Li, G., Worsnop, D. R., and O'Dowd, C. D.: Severe Pollution in China Amplified by Atmospheric
697 Moisture, Sci. Rep., 7, 10.1038/s41598-017-15909-1, 2017.
698 Tröstl, J., Chuang, W. K., Gordon, H., Heinritzi, M., Yan, C., Molteni, U., Ahlm, L., Frege, C., Bianchi,

https://doi.org/10.5194/acp-2020-792
Preprint. Discussion started: 25 August 2020

Atmospheric Chemistry and Physics Discussions

F., Wagner, R., Simon, M., Lehtipalo, K., Williamson, C., Craven, J. S., Duplissy, J., Adamov, A., Almeida, J., Bernhammer, A.-K., Breitenlechner, M., Brilke, S., Dias, A., Ehrhart, S., Flagan, R. C., Franchin, A., Fuchs, C., Guida, R., Gysel, M., Hansel, A., Hoyle, C. R., Jokinen, T., Junninen, H., Kangasluoma, J., Keskinen, H., Kim, J., Krapf, M., Kürten, A., Laaksonen, A., Lawler, M., Leiminger, M., Mathot, S., Möhler, O., Nieminen, T., Onnela, A., Petäjä, T., Piel, F. M., Miettinen, P., Rissanen, M. P., Rondo, L., Sarnela, N., Schobesberger, S., Sengupta, K., Sipilä, M., Smith, J. N., Steiner, G., Tomè, A., Virtanen, A., Wagner, A. C., Weingartner, E., Wimmer, D., Winkler, P. M., Ye, P., Carslaw, K. S., Curtius, J., Dommen, J., Kirkby, J., Kulmala, M., Riipinen, I., Worsnop, D. R., Donahue, N. M., and Baltensperger, U.: The role of low-volatility organic compounds in initial particle growth in the atmosphere, Nature, 533, 527-531, 10.1038/nature18271, 2016.

Ulbrich, I. M., Canagaratna, M. R., Zhang, Q., Worsnop, D. R., and Jimenez, J. L.: Interpretation of organic components from positive matrix factorization of aerosol mass spectrometric data, Atmos. Chem. Phys., 9, 2891-2918, 10.5194/acp-9-2891-2009, 2009.

Wang, G., Zhang, R., Gomez, M. E., Yang, L., Levy Zamora, M., Hu, M., Lin, Y., Peng, J., Guo, S., Meng, J., Li, J., Cheng, C., Hu, T., Ren, Y., Wang, Y., Gao, J., Cao, J., An, Z., Zhou, W., Li, G., Wang, J., Tian, P., Marrero-Ortiz, W., Secrest, J., Du, Z., Zheng, J., Shang, D., Zeng, L., Shao, M., Wang, W., Huang, Y., Wang, Y., Zhu, Y., Li, Y., Hu, J., Pan, B., Cai, L., Cheng, Y., Ji, Y., Zhang, F., Rosenfeld, D., Liss, P. S., Duce, R. A., Kolb, C. E., and Molina, M. J.: Persistent sulfate formation from London Fog to Chinese haze, Proc. Natl. Acad. Sci. USA, 113, 13630-13635, 10.1073/pnas.1616540113, 2016.

Wang, Q., Sun, Y., Xu, W., Du, W., Zhou, L., Tang, G., Chen, C., Cheng, X., Zhao, X., Ji, D., Han, T., Wang, Z., Li, J., and Wang, Z.: Vertically resolved characteristics of air pollution during two severe winter haze episodes in urban Beijing, China, Atmos. Chem. Phys., 18, 2495-2509, 10.5194/acp-18-

https://doi.org/10.5194/acp-2020-792
Preprint. Discussion started: 25 August 2020

721 2495-2018, 2018.

722 Wang, Y. C., Huang, R. J., Ni, H. Y., Chen, Y., Wang, Q. Y., Li, G. H., Tie, X. X., Shen, Z. X., Huang, Y.,
723 Liu, S. X., Dong, W. M., Xue, P., Fröhlich, R., Canonaco, F., Elser, M., Daellenbach, K. R., Bozzetti, C.,
724 El Haddad, I., Prévôt, A. S. H., Canagaratna, M. R., Worsnop, D. R., and Cao, J. J.: Chemical composition,
725 sources and secondary processes of aerosols in Baoji city of northwest China, Atmos. Environ., 158, 128-
726 137, https://doi.org/10.1016/j.atmosenv.2017.03.026, 2017.

727 Wu, Y., Ge, X., Wang, J., Shen, Y., Ye, Z., Ge, S., Wu, Y., Yu, H., and Chen, M.: Responses of secondary
728 aerosols to relative humidity and photochemical activities in an industrialized environment during late
729 winter, Atmos. Environ., 193, 66-78, 10.1016/j.atmosenv.2018.09.008, 2018.

730 Xie, Q., Li, Y., Yue, S., Su, S., Cao, D., Xu, Y., Chen, J., Tong, H., Su, H., Cheng, Y., Zhao, W., Hu, W.,
731 Wang, Z., Yang, T., Pan, X., Sun, Y., Wang, Z., Liu, C.-Q., Kawamura, K., Jiang, G., Shiraiwa, M., and
732 Fu, P.: Increase of High Molecular Weight Organosulfate With Intensifying Urban Air Pollution in the
733 Megacity Beijing, J. Geophys. Res. Atmos., 125, e2019JD032200, 10.1029/2019jd032200, 2020.

734 Xu, J., Zhang, Q., Chen, M., Ge, X., Ren, J., and Qin, D.: Chemical composition, sources, and processes
735 of urban aerosols during summertime in northwest China: Insights from high-resolution aerosol mass
736 spectrometry, Atmos. Chem. Phys., 14, 12593-12611, 10.5194/acp-14-12593-2014, 2014.

737 Xu, J., Shi, J., Zhang, Q., Ge, X., Canonaco, F., Prévôt, A. S. H., Vonwiller, M., Szidat, S., Ge, J., Ma, J.,
738 An, Y., Kang, S., and Qin, D.: Wintertime organic and inorganic aerosols in Lanzhou, China: Sources,
739 processes, and comparison with the results during summer, Atmos. Chem. Phys., 16, 14937-14957,
740 10.5194/acp-16-14937-2016, 2016.

741 Xu, Q., Wang, S., Jiang, J., Bhattarai, N., Li, X., Chang, X., Qiu, X., Zheng, M., Hua, Y., and Hao, J.:
742 Nitrate dominates the chemical composition of $PM_{2.5}$ during haze event in Beijing, China, Sci. Total

https://doi.org/10.5194/acp-2020-792
Preprint. Discussion started: 25 August 2020

743 Environ., 689, 1293-1303, 10.1016/j.scitotenv.2019.06.294, 2019a.

744 Xu, W., Han, T., Du, W., Wang, Q., Chen, C., Zhao, J., Zhang, Y., Li, J., Fu, P., Wang, Z., Worsnop, D.
745 R., and Sun, Y.: Effects of aqueous-phase and photochemical processing on secondary organic aerosol
746 formation and evolution in Beijing, China, Environ. Sci. Technol., 51, 762-770, 10.1021/acs.est.6b04498,
747 2017.

748 Xu, W., Sun, Y., Wang, Q., Zhao, J., Wang, J., Ge, X., Xie, C., Zhou, W., Du, W., Li, J., Fu, P., Wang, Z.,
749 Worsnop, D. R., and Coe, H.: Changes in aerosol chemistry from 2014 to 2016 in winter in Beijing:
750 Insights from high-resolution aerosol mass spectrometry, J. Geophys. Res. Atmos., 124, 1132-1147,
751 10.1029/2018jd029245, 2019b.

752 Yang, Y., Shao, M., Keßel, S., Li, Y., Lu, K., Lu, S., Williams, J., Zhang, Y., Zeng, L., Nölscher, A. C.,
753 Wu, Y., Wang, X., and Zheng, J.: How the OH reactivity affects the ozone production efficiency: case
754 studies in Beijing and Heshan, China, Atmos. Chem. Phys., 17, 7127-7142, 10.5194/acp-17-7127-2017,
755 2017.

756 Ye, Z., Li, Q., Liu, J., Luo, S., Zhou, Q., Bi, C., Ma, S., Chen, Y., Chen, H., Li, L., and Ge, X.:
757 Investigation of submicron aerosol characteristics in Changzhou, China: Composition, source, and
758 comparison with co-collected $PM_{2.5}$, Chemosphere, 183, 176-185, 10.1016/j.chemosphere.2017.05.094,
759 2017.

760 Yuan, B., Shao, M., de Gouw, J., Parrish, D. D., Lu, S., Wang, M., Zeng, L., Zhang, Q., Song, Y., Zhang,
761 J., and Hu, M.: Volatile organic compounds (VOCs) in urban air: How chemistry affects the interpretation
762 of positive matrix factorization (PMF) analysis, J. Geophys. Res. Atmos., 117, 10.1029/2012jd018236,
763 2012.

764 Zhang, J. K., Sun, Y., Liu, Z. R., Ji, D. S., Hu, B., Liu, Q., and Wang, Y. S.: Characterization of submicron

https://doi.org/10.5194/acp-2020-792
Preprint. Discussion started: 25 August 2020

Atmospheric Chemistry and Physics Discussions

765 aerosols during a month of serious pollution in Beijing, 2013, Atmos. Chem. Phys., 14, 2887-2903,
766 10.5194/acp-14-2887-2014, 2014.
767 Zhang, Q., Jimenez, J. L., Canagaratna, M. R., Ulbrich, I. M., Ng, N. L., Worsnop, D. R., and Sun, Y.:
768 Understanding atmospheric organic aerosols via factor analysis of aerosol mass spectrometry: a review,
769 Anal. Bioanal. Chem., 401, 3045-3067, 10.1007/s00216-011-5355-y, 2011.
770 Zhang, Q., Zheng, Y., Tong, D., Shao, M., Wang, S., Zhang, Y., Xu, X., Wang, J., He, H., Liu, W., Ding,
771 Y., Lei, Y., Li, J., Wang, Z., Zhang, X., Wang, Y., Cheng, J., Liu, Y., Shi, Q., Yan, L., Geng, G., Hong, C.,
772 Li, M., Liu, F., Zheng, B., Cao, J., Ding, A., Gao, J., Fu, Q., Huo, J., Liu, B., Liu, Z., Yang, F., He, K.,
773 and Hao, J.: Drivers of improved $PM_{2.5}$ air quality in China from 2013 to 2017, Proc. Natl. Acad. Sci.
774 USA, 116, 24463-24469, 10.1073/pnas.1907956116, 2019.